A Novel Lightweight Model for the Detection of COVID-19 and Other Lung Diseases

Shubham Dodia
Computer Engineering Department,VIIT
BRACT's Vishwakarma Institute of Information Technology,Pune
(of Affiliation)
Pune, India
Email: shubham.dodia@viit.ac.in

Naziya Mahimkar
Computer Engineering Department,VIIT
BRACT's Vishwakarma Institute of Information Technology,Pune
(of Affiliation)
Pune, India
Email: naziyamahimkar13@gmail.com

Yashraj Patil
Computer Engineering Department,VIIT
BRACT's Vishwakarma Institute of Information Technology,Pune
(of Affiliation)
Pune, India
Email: yashraj.22111057@viit.ac.in

Harshada Navale
Computer Engineering Department,VIIT
BRACT's Vishwakarma Institute of Information Technology,Pune
(of Affiliation)
Pune, India
Email: harshdanavale2003@gmail.com

Mohsin Miyaji
Computer Engineering Department,VIIT
BRACT's Vishwakarma Institute of Information Technology,Pune
(of Affiliation)
Pune, India
Email: mohsin.22110061@viit.ac.in

Abstract— **The COVID-19 pandemic has highlighted the need for rapid and reliable diagnostic methods. Traditional testing approaches, such as RT-PCR and antigen tests, faced limitations in terms of speed and accuracy. False negatives exacerbated the challenges of containing the virus's spread, and the scarcity of test kits further strained healthcare systems worldwide. To address these challenges, researchers have turned to artificial intelligence, specifically convolutional neural networks (CNN), to diagnose COVID-19 using chest X-ray images. This research aimed to develop an AI-based diagnostic tool that not only identifies COVID-19 but also differentiates it from other lung ailments, such as viral pneumonia, and accurately classifies normal chest X-rays. The study utilized a large repository of chest X-ray images, comprising over 21,000 images from 15,000 patient cases. The research introduced a lightweight CNN model called "ShallowNet" to address resource efficiency and time optimization. The framework attained high accuracy rates for training, validation, and testing, showcasing the potential of this innovative approach as an effective diagnostic tool.**

Keywords—COVID-19, Lung diseases, Neural Network.

I. INTRODUCTION

The genesis of the COVID-19 pandemic can be traced back to the first documented pneumonia case with unclear etiology in Wuhan, China, in December 2019, marking the initial alarm of a global health crisis. Coronaviruses were first identified in humans in 1960. A specific strain, SARS-CoV, emerged in 2003. It is speculated that certain species of bats serve as a potential means through which this virus is transmitted to humans. SARS-CoV-2, later named COVID-19 by the WHO, was officially proclaimed as a worldwide epidemic in March 2020 [1]. There is a consensus that the virus probably emerged from bats and subsequently spread to humans through an intermediate animal host, possibly a species of pangolin [2].India being one of the densest and heavily populated countries of the world faced several waves of COVID-19 infections, with the most devastating wave occurring in the spring of 2021 [3]. From January 3, 2020 to October 4, 2023, there were 44,998,838 documented cases of COVID-19 in India, including 532,032 deaths reported to the World Health Organization. [4].

RT-PCR is the main diagnostic method for COVID-19. It's a powerful tool used to amplify and detect RNA molecules, commonly used in virology, genetics, and gene expression analysis. It's widely used in clinical diagnostics for infectious diseases caused by RNA viruses, genetic disorders, and monitoring gene expression changes in diseases. [5]. The process is hand-held, intricate, demanding in labor, and time-intensive, yielding a positivity rate of only 63%. Furthermore, a notable scarcity in its availability results in delays in implementing disease prevention measures.

A study revealed that individuals who survived COVID-19 pneumonia, the primary lung ailment resulting from the infection, began exhibiting alterations in 10 days from the onset of symptoms on their CT scan images [6]. CT scans and X-rays can detect lung abnormalities caused by COVID-19, which is crucial for treatment decisions and hospitalization. In certain places with limited rRT-PCR kits, China recommends relying on clinical and computed tomography findings of the thorax. [7]. CT scans are the main tool for identifying and handling COVID-19 pneumonia. When RT-PCR screening yields a negative result, CT scans can help detect lung abnormalities. [8].

CNN-based techniques using CT scans and X-ray pictures for COVID-19 detection have shown promising results. However, they should not replace appropriate testing procedures and need further research and development before commercial application. Many data scientists and researchers are working on enhancing deep machine learning for accurate COVID-19 detection.

II. DATASET

In this conducted study, we utilized an openly available large dataset comprising X-ray pictures of the thorax. The collected data was a collaborative effort between scientists from Qatar, Doha, and Bangladesh. It includes in total 21,165 X-ray visuals obtained from more than 15,000 patient cases. The dataset is categorized into four main classes:

1. 3,616 COVID cases
2. 1,345 Viral Pneumonia cases
3. 10,192 Normal cases
4. 6,012 Lung Opacity

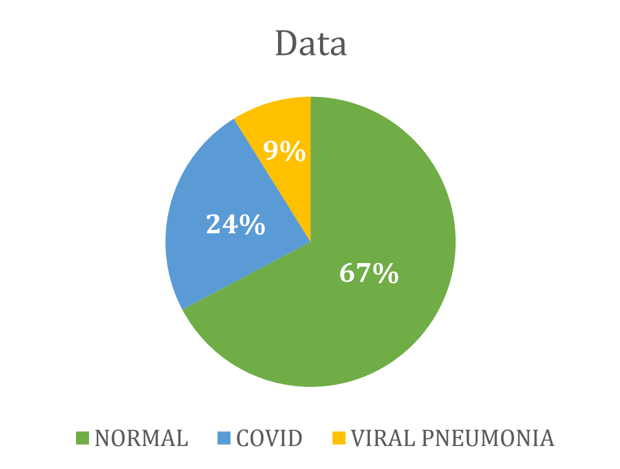

Fig 1. Pie chart of dataset used

The X-ray pictures of the chest were taken using the posterior-to-anterior (PA) and anterior-to-posterior (AP) views, which are commonly used in clinical diagnosis.

Major sources were used for the creation of the database used in this study. For more detailed information on the data collection process, patient demographics, and other dataset characteristics, please refer to the original research paper [16][17] where the dataset was first introduced.

Table 1. Number of images with augmentation used

STATISTICS OF DATA USED IN TRAINING THE MODEL					
CLASS	Total augmented Images	Used Images	Training Set	Validation set	Test set
COVID-19	3616	3616	3254	73	289
Normal	10192	10192	9172	204	816
Viral Pneumonia	1345	1345	1210	27	108
Total	**15,153**	**15,153**	**13,636**	**304**	**1213**

III. LITERATURE REVIEW

In the medical realm, numerous studies and methodologies have emerged in response to COVID-19. In this section, we cover a few of them.

Researchers have performed segmentation on lung X-ray images using a U-Net model to focus on only the lungs and not the surroundings. Arias-Garzón et al [9] used the modality VGG19 and UNet. The sample size consisted of frontal images – 2481, and lateral images – 815 for the classification model. The authors meticulously crafted a strategy to compare the effectiveness of preprocessing. Interestingly, the study emphasizes the utility of existing models for multiple tasks, highlighting that modified U-Net models did not outperform the baseline. Additionally, the research underscores the impact of image noise in introducing bias to the models. Muhammed Yildrim et al [10] employed SVM and KNN classifiers to investigate the potential confusion between imaging findings of COVID-19 pneumonia and other pneumonia cases. Their primary objective was to identify and distinguish COVID-19 pneumonia amidst instances of viral pneumonia.

The YOLO real-time object detection system, employing the DarkNet model as a classifier, features 19 convolution layers and 5 pooling layers utilizing Maxpool. Tulin Ozlurk et al [11] utilized a dataset with both binary and three-class classifications. The former included 125 COVID-19 cases and 500 No-findings. The latter consisted of 125 COVID-19, 500 pneumonia, and 500 No-findings. The proposed system demonstrated impressive performance on binary and multi-classification tasks. Md Mamunur et al [12] compared and studied 15 different models and found that VGG19 came out to be the most accurate. Using a dataset including 860 images they achieved the highest accuracy of 100%. To conclude VGG19 is the best CNN model for transfer learning.

In a study by Boran Sekeroglu et al [13], an analysis of various models including VGG19, ResNet50, VGG16, MobileNet-V2, Densenet121, SVM, KNN, LR, Naive Bayes, InceptionV3, and Decision Tree classifiers revealed that a CNN with reduced convolutional and fully connected layers displayed significant capability in accurately identifying COVID-19 images within binary classifications: COVID-19 with Normal cases; and COVID-19 with Pneumonia. Wesam atef et al [14] used the ResNet VGG and InceptionNet modality. Their dataset consisted of 30882 images of chest x-rays, 14192 non-covid, and 16690 covid. Their accuracy was 95.29% and found VGG16 to give the best accuracy.

In the study conducted by Emtiaz Hussaina et al. [15], they utilized a CNN-based classifier named CoroDet. Their experimental findings suggest that CoroDet outperforms existing state-of-the-art methods. The achieved accuracies were remarkable, with 99.1% for the two-class classification, 94.2% for the three-class classification, and 91.2% for the four-class classification. Muhammad E. H. Chowdhury et al [16] concluded that DenseNet201 and ChesXnet were the most accurate model. Both were deep-layer models and performed well with larger datasets. The sample size was 6540 and the VGG19 model was used. Accuracy came to be 99.7% for two class classifications.

IV. METHODOLOGY

In this section, the methodology behind creating & training the convolutional model is explored, covering the following aspects: Convolutional Neural Network (CNN), Transfer Learning, Proposed Model Architecture, Layers, Custom Activation Function, Trainable Parameters, and Final Output.

A. Convolutional Neural Network

A CNN architecture comprises three key elements:

- Convolutional layers
- Pooling layers
- Fully connected layer

CNN is a family of neural networks specially designed for processing visual data such as images and videos.

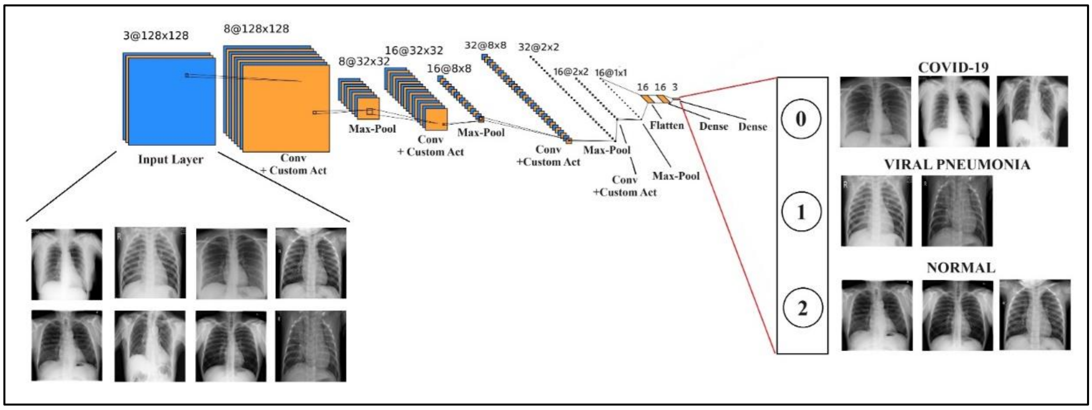

Fig 2. Visual representation detailing convolution and Max-pooling layer operations

B. Proposed Model Architecture

Our novel CNN model, named "ShallowNet", has been designed to address the pressing issue of resource efficiency and time optimization that conventional Transfer Learning COVID models struggle with. By meticulously reducing the number of trainable parameters and using a custom activation function, ShallowNet succeeds in streamlining the utilization of resources without compromising on performance standards. The diagrammatic view of the model is in figure 2.

C. Layers

ShallowNet comprises a concise architecture featuring seven trainable layers which are four Convolutional Layers, four Max-Pooling Layers, and three fully connected Layer. Designed for simplicity and resource optimization, ShallowNet takes an input image of 128 x 128 pixels with three color channels (RGB). In contrast to complex pre-trained models, ShallowNet is tailored to minimize computational demands, making it an excellent choice for applications where speed and efficiency are paramount and complexity requirement is less. It is an ideal model for rapid Image analysis.This model starts with an input image of 128 x 128 pixels and three color channels (RGB).

Table 2. Description of trainable parameters, number of filters, kernel size, strides and activation function used in each layer.

SHALLOWNET MODEL SUMMARY					
Layer (Type)	**Output Shape**	**Para-mete-rs**	**No. of Filt -ers**	**Kernel Size & Strides**	**Activation Function**
Input Layer	(128, 128, 3)	0	-	-	-
Conv2D_1	(128, 128, 8)	392	8	(4, 4) (1, 1)	Custom Activation
MaxPooling2 D_1	(32, 32, 8)	-	-	(8, 8) (4, 4)	-
Conv2D_2	(32, 32, 16)	528	16	(2, 2) (1, 1)	Custom Activation
MaxPooling2 D_2	(8, 8, 16)	-	-	(4, 4) (4, 4)	-
Conv2D_3	(8, 8, 32)	8224	32	(4, 4) (1, 1)	Custom Activation
MaxPooling2 D_3	(2, 2, 32)	-	-	(4, 4) (4, 4)	-
Conv2D_4	(2, 2, 16)	2064	16	(2, 2) (1, 1)	Custom Activation
MaxPooling2 D_4	(1, 1, 16)	-	-	(4, 4) (4, 4)	-
Flatten	(16)	-	-	-	-
Dense_1	(16)	272	-	-	tanh
Dense_2	(3)	51	-	-	softmax

The reduction in x and y dimensions as we delve deeper into the model helps in capturing and emphasizing only the most critical features of the image. This selective feature extraction enables ShallowNet to discard unimportant and less relevant details, resulting in a lean and efficient representation of the input image. Layer-by-layer information is given in Table 2.

D. Custom Activation Function

In our study, we introduced a new custom activation function defined in equation 1.

$$y = \max\left(0, \frac{x}{x + e^{-x}}\right) \qquad \textbf{(1)}$$

This custom activation function as seen in figure 3 is specifically designed to address several key issues with traditional activation functions commonly used in neural networks. The main advantage of the adaptive activation function is its smooth and separable nature, which ensures the computability of gradients for efficient backpropagation during training, which is crucial for neural network optimization. Our custom activation function, like the sigmoid, has a range of (0, 1), which reduces the risk of exploding gradients for large positive inputs. This is in sharp contrast to ReLU, which goes from zero to positive infinity, which can lead to the problem of explosive gradients, especially in deep networks. By zeroing out negative activations, it introduces sparsity in the network, resulting in more efficient representations and quicker convergence during training.

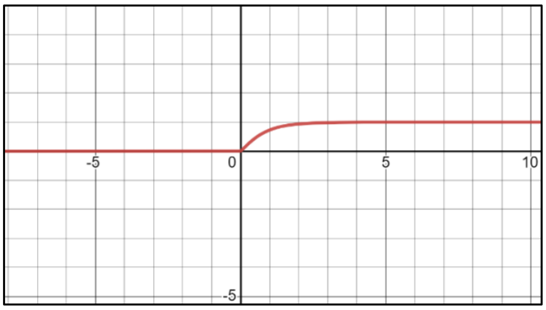

Fig 3. Graphical view of proposed custom activation function

In our experiments, our neural network model using the custom activation function outperformed its counterpart using ReLU as the activation function, highlighting the superiority of the custom activation function over the proposed model. This custom activation function not only overcomes the limitations of traditional activation functions but also provides improved performance, making it a valuable addition to the arsenal of activation functions in neural network design.

E. Trainable Parameters and Output

ShallowNet is exceptionally lightweight, boasting a total of just 11,531 trainable parameters. This minimal parameter count significantly reduces training time and model size. It's an ideal choice when efficiency is a priority. The model produces its output through a softmax activation function. In the output, the label "0" corresponds to COVID-19, "1" signifies viral pneumonia, and "2" represents normal cases. This clear and straightforward output encoding simplifies result interpretation, making it a practical choice for classification tasks.

V. TRAINING AND TESTING

For training the initial Learning Rate was 0.0006, decay rate 1, and decay step 10. The model used an exponential learning rate decay function. This technique allowed the model to adjust its learning rate over time, helping it converge to an optimal solution. For optimization, the model used the Adam optimization algorithm. To prevent overfitting, early stopping was implemented, ensuring the model's generalization capacity. Each training batch consisted of 32 images, and the model was trained over the course of 21 epochs. Training for each epoch took approximately one minute, with the entire process lasting 22 minutes. The model's final training accuracy reached an impressive 98.22%, indicating its ability to fit the training data closely.

Furthermore, the model displayed strong generalization capabilities, achieving a validation accuracy of 94.74%. In a real-world scenario, this performance metric is of great importance, as it gauges the model's ability to make accurate predictions on previously unseen data. When subjected to the test set, the model performed well by attaining a testing accuracy of 95.96%. This result indicates the model's competence in handling new, unfamiliar data, an essential aspect of its practical utility.

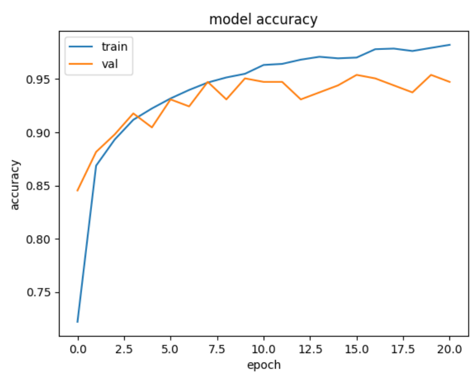

Fig 4. Accuracy vs. epoch graph for train and validation set

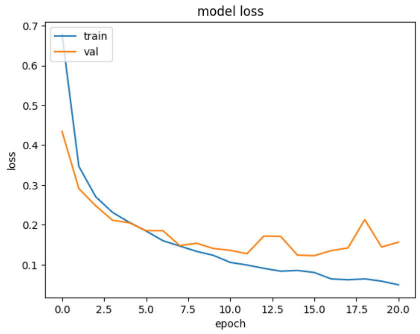

Fig 5. Loss vs. epoch graph for train and validation set

Figure 4 shows the accuracy versus epoch graph for train validation set. In the initial epochs the training accuracy increases steadily this indicates that the model is learning from the initial data and is becoming better at making predictions as it is gaining more experience. As the epochs progress, both training and validation accuracy show simultaneous improvement. The small consistent gap between validation accuracy the training accuracy signifies that the model is well-generalized and is effectively learning from the data and not merely memorizing it. Both training and validation accuracy plateau at an elevated level.

In the loss vs. epoch graph in figure 5, both training and validation losses exhibit a gradual decline as the number of epochs increases. This decreasing trend in loss values signifies that the model is actively learning and refining its parameters to better align with the training data. The integration of early stopping as a preventive measure ensures that the model does not excessively tailor itself to the training data, thus guarding against overfitting.

VI. RESULTS

This section contains the findings from the testing conducted on the proposed model "ShallowNet". We employed a custom CNN model with a unique activation function and compared its performance with two pre-built architectures, VGG16 and AlexNet. Additionally, we assessed the impact of using the standard ReLU activation function on the CNN model's performance.

We trained our custom CNN model with the unique activation function on a dataset comprising pictures of chest X-rays and achieved impressive results in terms of accuracy, precision, recall, and F1 score. The performance metrics for our custom model are shown in Table 3.

Table 3. Comparison table between VGG-16, AlexNet, and proposed model.

Model	Accuracy	Precision	Recall	F1-Score
VGG-16	84%	85%	88%	86%
AlexNet	72%	74%	64%	67%
Proposed Model	96%	95%	94%	95%

Table 4. State-of-the-Art in COVID-19 Classification Using Chest X-Ray Images

Articles	Techniques	Dataset	Accuracy
Tsung et al. [**19**]	CNN (ResNet50)	15478 chest X-ray images (473 COVID)	93.1%
Emtiaz et al. [**15**]	CoroDet(CNN based classifier)	2100 chest X-ray images (500 COVID)	94.2%
Morteza et al. [**20**]	VGG16 + 2-step preprocessing	8474 chest X-ray images (415 COVID)	94.5%
Tulin et al. [**11**]	DarkCovidNet	1125 Chest X-ray images (125 COVID)	87.02%
Ioannis et al. [**18**]	VGG-19	1428 Chest X-ray (224 COVID, 700 Pneumonia, 504 Healthy)	93.48%
Xu et al. [**21**]	ResNet + Location Attention	618 Chest CT (219 COVID, 224 Viral pneumonia, 175 Healthy)	86.7%
Proposed Model	**ShallowNet**	**15153 Chest X-ray images (3616 COVID)**	**95.96%**

The performance of VGG16 and AlexNet, while respectable, was notably lower compared to our custom model. It is important to highlight that the custom model outperformed both VGG16 and AlexNet in all performance metrics, demonstrating the significance of tailoring the model architecture for the specific task. Table 4 provides a comprehensive comparison of the performance metrics between our custom CNN model with other similar studies.

To further investigate the impact of the activation function on our custom CNN model's performance, we also trained the model using the standard ReLU activation function. The findings can be found in Table 5:

- **Accuracy of Custom Activation**: 95.96%
- **Accuracy of Relu Activation:** 90%

Table 5. Performance Evaluation of Custom Activation vs. ReLU Activation Models

Model	**Type**	**Precision**	**Recall**	**F1-score**
Proposed Model with Relu Activation	COVID	80%	86%	83%
	Viral Pneumonia	92%	90%	91%
	Normal	95%	92%	93%
	Average	89%	89%	89%
Proposed Model with Custom Activation	COVID	93%	92%	93%
	Viral Pneumonia	94%	94%	94%
	Normal	97%	97%	97%
	Average	95%	94%	95%

When comparing these results with the custom CNN model's performance using the unique activation function, it is evident that the custom activation function yields superior results. The custom activation function achieved almost 6% higher accuracy. While the model with the ReLU activation function exhibited good performance, it fell short in comparison to the custom activation function variant. This finding reinforces the importance of activation function design in optimizing the model for COVID-19 detection from chest X-ray images. The state-of-the-art comparison is been visually depicted in Figure 6.

The confusion matrix in Figure 7 summarizes the results of the whole model. It signifies the model is not biased to a particular class and hence serves its purpose.

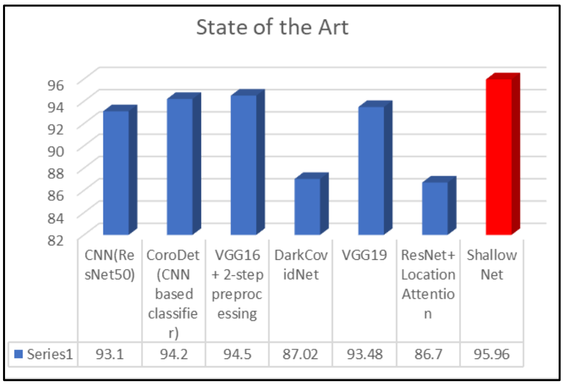

Fig 6. A bar chart comparing the accuracy of different COVID–19 classification models.

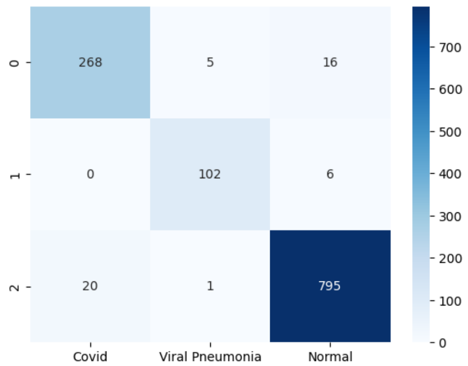

Fig. 7 Confusion matrix for each fold in 3 class classification.

VII. CONCLUSION

In conclusion, the utilization of X-ray imaging in the detection of COVID-19 has proven to be a valuable tool in the diagnosis and monitoring of this infectious disease. This research gives us hope by showing an accuracy of 95.96% on the dataset. Using deep learning can make diagnosing COVID-19 faster and more accurate. By utilizing the power of deep learning models, including "ShallowNet", the model conducts an extensive examination of these images. It excels in distinguishing COVID-19 from other pneumonia diseases, surpassing alternative methods. It could help doctors find cases of COVID-19 quickly and avoid making mistakes. This AI method is a valuable tool for healthcare workers in the fight against the pandemic, helping them do their jobs better and faster.

VIII.REFERENCES

[1] Cucinotta D, Vanelli M. WHO Declares COVID-19 a Pandemic. Acta Biomed. 2020 Mar 19;91(1):157-160. doi: 10.23750/abm.v91i1.9397. PMID: 32191675.

[2] Gupta SK, Minocha R, Thapa PJ, Srivastava M, Dandekar T. Role of the Pangolin in Origin of SARS-CoV-2: An Evolutionary Perspective. Int J Mol Sci. 2022 Aug 14;23(16):9115.

[3] Times of India (2020 September 4), *Covid-19: Over 83,000 cases, India sees new high;* http://timesofindia.indiatimes.com/articleshow/77921767.cms?utm_source=contentofinterest&utm_medium=text&utm_campaign=cppst.

[4] WHO (2023 October 17), India Situation, http://covid19.who.int/region/searo/country/in.

[5] Emery SL, et al. Real-time reverse transcription-polymerase chain reaction assay for SARS-associated coronavirus. Emerg Infect Dis. 2004 Feb;10(2):311-6. doi: 10.3201/eid1002.030759. PMID: 15030703.

[6] Pan F, Ye T, Sun P, Gui S, Liang B, Li L, et al. 2020 Time Course of Lung Changes at Chest CT during Recovery from Coronavirus Disease 2019 (COVID-19). Radiology. 295(3): 715–721.

[7] Chunqin Long, Hglin Shen, Xianghai Zhang, Bing Fan, Chuanhong Wang, et al. Diagnosis of the Coronavirus disease (COVID-19): rRT-PCR or CT?, European Journal of Radiology, Volume 126, 2020, 108961, ISSN 0720-048X.

[8] Zhao W, Zhong Z, Xie X, Yu Q, Liu J. Relation between chest CT findings and clinical conditions of coronavirus disease (COVID-19) pneumonia: a multi-center study. AJR 2020; 214:1072–1077, doi: 10.2214/AJR.20.22976

[9] Daniel Arias-Garzón, Jesús Alejandro Alzate-Grisales, Simon Orozco-Arias, Bravo-Ortiz, Alejandro Mora-Rubio, et al. COVID-19 detection in X-ray images using convolutional neural networks, Machine Learning with Applications, Volume 6, 2021, 100138, ISSN 2666-8270.

[10] Yildirim, M., Eroğlu, O., Eroğlu, Y. et al. COVID-19 Detection on Chest X-ray Images with the Proposed Model Using Artificial Intelligence and Classifiers. New Gener. Computer. 40, 1077–1091 (2022).

[11] Tulin Ozturk, Muhammed Talo, U. Rajendra Acharya, Automated detection of COVID-19 cases using deep neural networks with X-ray images, Computers in Biology and Medicine, Volume 121, 2020, 103792.

[12] Rahaman MM, Li C, Yao Y, Kulwa F, Rahman MA, Wang Q, et al. Identification of COVID-19 samples from chest X-Ray images using deep learning: A comparison of transfer learning approaches. J Xray Sci Technol. 2020;28(5):821-839.

[13] Sekeroglu B, Ozsahin I. Detection of COVID-19 from Chest X-Ray Images Using Convolutional Neural Networks. SLAS TECHNOLOGY: Translating Life Sciences Innovation. 2020;25(6):553-565. doi:10.1177/2472630320958376

[14] Wesam Atef Hatamleh, Hussam Tarazi, Chatti Subbalakshmi, Basant Tiwari, "Analysis of Chest X-Ray Images for the Recognition of COVID-19 Symptoms Using CNN", Wireless Communications and Mobile Computing, vol. 2022, Article ID 3237361, 12 pages, 2022.

[15] Emtiaz Hussain, Mahmudul Hasan, Md Anisur Rahman, Ickjai Lee, Tasmi Tamanna, Mohammad Zavid Parvez, CoroDet: A deep learning based classification for COVID-19 detection using chest X-ray images, Chaos, Solitons & Fractals, Volume 142, 2021, 110495, ISSN 0960-0779.

[16] M. E. H. Chowdhury et al., "Can AI Help in Screening Viral and COVID-19 Pneumonia?," in IEEE Access, vol. 8, pp. 132665-132676, 2020, doi: 10.1109/ACCESS.2020.3010287

[17] Tawsifur Rahman, Amith Saad Bin Abul Kashem, et al. Exploring the effect of image enhancement techniques on COVID-19 detection using chest X-ray images, Computers in Biology and Medicine, Volume 132, 2021, 104319, ISSN 0010-4825.

[18] Ioannis D. Apostolopoulos, Tzani Bessiana, "Covid-19: Automatic detection from X-Ray images utilizing Transfer Learning with Convolutional Neural Networks," Phys. Eng. Sci. Med., vol. 43, no. 6, pp. 635-640, Apr. 2020.

[19] Tsung-Chieh Lin and Hsi-Chieh Lee. 2020. Covid-19 Chest Radiography Images Analysis Based on Integration of Image Preprocess, Guided Grad-CAM, Machine Learning and Risk Management. In Proceedings of the 4th ICMHI '20. Association for Computing Machinery, NY, USA, 281–288.

[20] Heidari M, Mirniaharikandehei S, Khuzani AZ, Danala G, Qiu Y, Zheng B. Improving the performance of CNN to predict the likelihood of COVID-19 using chest X-ray images with preprocessing algorithms. Int J Med Inform. 2020 Dec;144:104284.

[21] Xiaowei Xu, Xiangao Jiang, Chunlian Ma, Peng Du, Xukun Li, Shuangzhi Lv, et al. "Deep Learning System to Screen Coronavirus Disease 2019 Pneumonia," Engineering, vol. 6, no. 10, pp. 1122-1129, October 2020.